0026-895X/04/6505-1120–1129$20.00
MOLECULAR PHARMACOLOGY
Copyright © 2004 The American Society for Pharmacology and Experimental Therapeutics
Mol Pharmacol 65:1120–1129, 2004

Vol. 65, No. 5
2934/1146848
Printed in U.S.A.

Molecular Determinants for High-Affinity Block of Human EAG Potassium Channels by Antiarrhythmic Agents

Guido Gessner, Martin Zacharias, Susanne Bechstedt, Roland Schönherr, and Stefan H. Heinemann

Research Unit Molecular and Cellular Biophysics, Medical Faculty of the Friedrich Schiller University Jena, Jena, Germany (G.G., S.B., R.S., S.H.H.); and School of Engineering and Sciences, International University Bremen, Bremen, Germany (M.Z.)

Received September 3, 2003; accepted February 3, 2004

This article is available online at http://molpharm.aspetjournals.org

ABSTRACT

Undesired block of human ERG1 potassium channels is the basis for cardiac side effects of many different types of drugs. Therefore, it is important to know exactly why some drugs particularly bind to these channels with high affinity. Upon expression in mammalian cells and *Xenopus laevis* oocytes, we investigated the inhibition of the closely related hEAG1 and hEAG2 channels by agents that have previously been reported to block hERG1 channels. Clofilium inhibited hEAG1 and hERG1 with the same potency, whereas hEAG2 was about 150-fold less sensitive to this antiarrhythmic agent. The molecular determinants for this difference are residues Ser436 and Val437 in the inner cavity of the pore and Ala453, which is located in S6 (i.e., remote from the inner cavity). A modeling approach that allowed for partial conformational relaxation of hEAG model structures upon ligand docking suggests that high-affinity block of *ether à go-go* channels is mediated by an anchoring of the clofilium alkane tail between S6 and the pore helices. In qualitative agreement with experiments, the mutations of hEAG1 residues Ser436 and Val437 to the corresponding larger hEAG2 residues (Thr432, Ile433) resulted in reduced sterical fit between the ligand and the binding cavity. The model is further supported by functional assays involving (+)-*N*-[1′-(6-cyano-1,2,3,4-tetrahydro-2(*R*)-naphthalenyl)-3,4-dihydro-4(*R*)-hydroxyspiro(2*H*-1-benzopyran-2,4′-piperidin)-6-yl]methanesulfonamide monohydrochloride (MK-499), terfenadine, quinidine, and tetrabutylammonium that are differentially affected by mutations in the pore pocket.

The EAG gene family consists of the EAG (*ether à go-go*), ERG (*ether à go-go*–related gene), and *ether à go-go*–like potassium channel subfamilies (Bauer and Schwarz, 2001), all of which encode depolarization-activated potassium (K^+) channels. hERG1 channels are predominantly expressed in the heart and give rise to the repolarizing I_{Kr} current that is responsible for action potential termination (Sanguinetti et al., 1995). Genetic defects in the *herg1* gene can cause the long-QT2 syndrome, which sometimes leads to sudden cardiac death. More common, however, are acquired forms of the long-QT syndrome, caused by the pharmacological blockade of cardiac ion channels. In this context, hERG1 channels seem to be the most important target for those substances that induce the undesired side effect of QT prolongation (Keating and Sanguinetti, 2001). Therefore, substantial effort is spent in elucidating the structural requirements that make hERG1 channels particularly susceptible to various agents, whereas most other voltage-gated K^+ channels (Kv channels) are insensitive. In a pioneering work by Mitcheson and colleagues (2000), an alanine scan of the inner pore region of hERG1 channels identified several residues that are of particular importance for stabilizing antiarrhythmic drugs inside the pore cavity. In the first place, these were two aromatic residues in the sixth transmembrane segment (Tyr652 and Phe656; see Fig. 2a) and two more residues facing the cavity at the apex of the pore helix (Thr623 and Val625). In particular the aromatic (S6) residues have been shown to be of high importance for hERG1 inhibition by a broad range of substances, including dofetilide, quinidine, MK-499, terfenadine, cisapride, vesnarinone, and chloroquine (Lees-Miller et al., 2000; Mitcheson et al., 2000; Kamiya et al., 2001; Sánchez-Chapula et al., 2002). However, they may constitute a necessary, but not a sufficient criterion for high-affinity block (nanomolar range) of antiarrhythmic agents.

This becomes evident in that the mentioned residues within S6 are conserved among EAG channels, although these channels differ strongly in their pharmacological properties. Schönherr et al. (2002) have shown that hEAG1 and

This work was supported by Deutsche Forschungsgemeinschaft grants HE 2993/6, SFB 604 TP A4 and B7.

ABBREVIATIONS: EAG, *ether à go-go*; ERG, *ether à go-go*–related gene potassium channel; HEK, human embryonic kidney; LY97241, *p*-nitro tertiary clofilium (*N*-ethyl-*N*-heptyl-4-nitrobenzene butanamine ethandioc acid salt; TBA, tetrabutylammonium; MK-499, (+)-*N*-[1′-(6-cyano-1,2,3,4-tetrahydro-2(*R*)-naphthalenyl)-3,4-dihydro-4(*R*)-hydroxyspiro(2H-1-benzopyran-2,4′-piperidin)-6-yl]methanesulfonamide monohydrochloride.

hEAG2 channels differ in their sensitivity toward the antiarrhythmic agent quinidine by a factor of ~100. Ju and Wray (2002) have shown that these channels differ in sensitivity toward terfenadine. Moreover, recent data indicate that the aromatic S6 residues Tyr652 and, in particular, Phe656 only partially affect hERG1 inhibition by fluvoxamine (Milnes et al., 2003).

Hence, the pharmacology of K^+ channels from the EAG family is not simply determined by residues of the central pore cavity. In this respect, hEAG1 and hEAG2 provide an ideal pair of highly conserved proteins with different pharmacological properties. Given the strong sensitivity of hEAG1 channels toward the quaternary ammonium derivative clofilium and its tertiary analog LY97241 (Gessner and Heinemann, 2003), we systematically investigated the differences of pharmacological properties of these two channels. Employing site-directed mutagenesis and electrophysiological characterization of the effects of various drugs on these channels we identified residues inside the channel's pore that are essential for high-affinity blockade. In addition to two sites in the cavity (Ser436 and Val437), the residue Ala453 was found to be important for high-affinity binding of clofilium by hEAG1. Our experimental findings could be qualitatively reproduced in a ligand docking approach, making use of hEAG homology models based on the crystal structure of the bacterial KcsA channel (Doyle et al., 1998). The docking simulations with partial conformational relaxation of the hEAG model structures suggest a high-affinity binding mode with the alkane tail of clofilium located between selectivity filter and S6 helix. This binding mode can also qualitatively explain the effect of amino acid differences between hEAG1 and hEAG2 on clofilium binding based on differences in stereo-chemical fit between ligand and receptor. We propose a binding mode of "anchored cavity block," which assumes that blocking molecules in the cavities can be anchored by hydrophobic chains in the space between the pore helix and S6, leading to increased binding affinity.

Materials and Methods

Molecular Biology

hEAG1 and hEAG2 were used in the vectors pGEM-HE (oocyte expression) and pcDNA3 (mammalian expression) as described previously (Schönherr et al., 2002). Chimeric channels in which either the entire membrane-spanning core domain (c) or the pore domain (p) was exchanged were constructed (see Fig. 2a). The chimeric protein with the core domain of hEAG2 embedded into cytoplasmic regions of hEAG1 (E1-c2) consists of amino acid residues 1 to 182 (hEAG1), 180 to 501 (hEAG2), and 506 to 962 (hEAG1). The complementary protein E2-c1 comprises residues 1 to 179 (hEAG2), 183 to 505 (hEAG1), and 502 to 988 (hEAG2). In a protein with the hEAG1 pore in the context of hEAG2 (E2-p1), residues 421 to 500 of hEAG2 were replaced by residues 425 to 504 from hEAG1. The complementary chimeric protein E1-p2 contains residues 421 to 500 from hEAG2 in place of residues 425 to 504 from hEAG1. Each pore chimera differs in nine amino acid positions from the respective native channel protein. These nine residues were replaced individually in hEAG1 by the corresponding residues of hEAG2, using overlap extension PCR (Ho et al., 1989). Individual amino acid replacements in hEAG1 are: S433A, S433C, S436T, V437I, S445T, I448V, I451M, A453S, I456M, M457A, I459V, and S491N. In hEAG2, the pore mutation T432S/I433V was generated. A fusion construct (E1-S5p2) encodes the outer pore region of hEAG2 (S5 end to pore helix; amino acids 371–420) in the background of hEAG1 (1–373 and 425–962). The triple mutant T432S/I433V/S449A was generated in the background of hEAG1 with the core domain of hEAG2 (E1-c2 TIS/SVA). hERG1 channels were used in a pcDNA3 vector (Gessner and Heinemann, 2003). Mutant S641A was introduced by standard methods.

Expression of hEAG and hERG Channels in HEK 293 Cells and *Xenopus laevis* Oocytes

HEK 293 cells were cultured in 45% Dulbecco's modified Eagle's medium, 45% Ham's F-12 medium (Invitrogen, Karlsruhe, Germany), and 10% fetal calf serum. Cells were maintained at 37°C in a humidified atmosphere with 5% CO_2 and subcultured every 3 to 4 days. For electrophysiological recordings cells were plated on 35-mm Petri dishes and transiently transfected using the Polyfect method (QIAGEN, Hilden, Germany).

For expression in *X. laevis* oocytes, capped mRNA was synthesized in vitro with the T7 mMESSAGE mMACHINE kit (Ambion, Austin, TX). Oocyte preparation and injection of RNA was performed as described previously (Schönherr and Heinemann, 1996).

Electrophysiological Recordings

We used an EPC 9 patch-clamp amplifier (HEKA Elektronik, Lambrecht, Germany). Patch pipettes for whole-cell recordings were fabricated from borosilicate glass (Kimble Glass, Vineland, NJ) with tip resistances of 1 to 2 MΩ. Pipettes were filled with 140 mM KCl, 10 mM EGTA, and 10 mM HEPES, pH 7.4 (adjusted with KOH). The standard bath solution contained 145 mM NaCl, 5 mM KCl, 2 mM $CaCl_2$, and 10 mM HEPES, pH 7.4 (NaOH). hERG1 currents were recorded in bath solutions with elevated K^+ concentration (40 mM; Gessner and Heinemann, 2003). Currents were measured in the whole-cell configuration with access resistances below 3 MΩ. Series resistance compensation was applied to 80 to 90%.

For macro-patch recordings from *X. laevis* oocytes in the inside-out configuration, the patch pipettes were formed from aluminum silicate glass (Hilgenberg, Malsfeld, Germany) with tip resistances of 1 to 2 MΩ. Standard external solution was composed of 103.6 mM sodium aspartate, 11.4 mM KCl, 1.8 mM CaCl2, and 10 mM HEPES, pH adjusted to 7.4 with NaOH. Standard internal solution contained 120 mM potassium aspartate, 15 mM KCl, 10 mM EGTA, and 10 mM HEPES, pH adjusted to 7.4 with KOH. Pipette tips for both types of experiments were fire-polished immediately before use. All experiments were performed at room temperature (20–23°C).

All chemicals used were of high grade, obtained from Sigma (Taufkirchen, Germany). LY97241 was kindly provided by Eli Lilly (Indianapolis, IN) and MK-499 by MSD Sharp and Dohme (Haar, Germany).

K^+ channel blockers were dissolved in the bath solution immediately before the experiments. They were applied to the cells/patches via complete exchange of the bath solution. Blocker effects were allowed to equilibrate, monitored during repetitive depolarizations. Current block was analyzed by plotting the remaining current, normalized to the control current before blocker application as a function of the blocker concentration. IC_{50} values were obtained by fitting a Hill equation to these data: $I/I_{control} = 1/[1 + ([blocker]/IC_{50})^{n_H}]$, where IC_{50} is the half-maximal inhibition concentration and n_H is the Hill coefficient.

To assay the voltage dependence of the channels, currents at the end of 1-s depolarizations to voltages between −70 and +60 mV were measured. Currents were converted to conductances (G) on the basis of the Goldman-Hodgkin-Katz equation, assuming a reversal potential of −85 mV, and fitted with a Boltzmann function: $G = G_{max}/(1 + \exp[(V_n - V)/k_n])$, where G_{max} is maximal conductance, V_n is the half-maximal activation voltage, and k_n is a slope factor that characterizes the voltage dependence. For better comparison, conductance-voltage relationships were normalized to G_{max} yielding open probabilities.

Data acquisition and analysis were carried out with

Pulse+PulseFit, PatchMaster (HEKA), and IgorPro (WaveMetrics, Lake Oswego, OR) software. All data are presented as mean ± S.E.M. (n), where n is the number of independent experiments.

Molecular Modeling

EAG Pore Models Based on KcsA Structure. Structural models of hEAG1 and hEAG2 were generated using the INSIGHT II program (Accelrys Inc., San Diego, CA) based on the sequence alignment shown in Fig. 3 and on the crystal structure of the bacterial KcsA K^+ channel (Doyle et al., 1998; Zhou et al., 2001) (Protein Data Bank code 195j). The side chain conformations of the generated model structures were checked manually for the best fitting possible rotamers. The structures were energy-minimized (500 steps) using the Sander module of the Amber program (Case et al., 1999). To avoid any large-scale conformational changes and because minimization was performed in the absence of explicit solvent, the protein backbone was weakly restrained to the template backbone structure (restraining force constant: 7 kcal mol^{-1} $Å^{-2}$). The protein backbone, as well as those side chains that are different in hEAG1 and 2, are shown in Fig. 3b.

Ligand Docking. A surface probe (1-Å radius) was used to map the boundaries of the putative ligand-binding cavity in front of the selectivity filter of the hEAG1 model structure. These boundaries served to guide initial random clofilium and quinidine ligand placements such that most ligand atoms were located within the boundaries and do not produce sterical clashes with protein atoms. The docked complexes were subsequently energy minimized with all ligand atoms free to move and either keeping the protein rigid (rigid docking) or allowing for some conformational readjustment with positional restraints on all protein atoms (semiflexible docking, restraining force constant: 10 kcal mol^{-1} $Å^{-2}$).

The recent crystal structure of the bacterial K^+ channel has been determined in complex with TBA (Zhou et al., 2001). However, the published structure deposited in the Protein Data Bank (code 195j) contains only coordinates for part of the TBA molecule (the tetraethylammonium core). Based on the observed ligand placement in the bacterial channel at the cavity in front of the selectivity filter, a putative complex between TBA and hEAG1 model was built (with the part of TBA that is identical to tetraethylammonium located at identical positions relative to the protein as found in the X-ray structure of the bacterial channel) and energy minimized.

To qualitatively evaluate the effect of amino acid changes in the hEAG1 model on interactions with ligands, the mutations were introduced using the BUILDER module of INSIGHT II. Complexes of the models with clofilium and quinidine were energy minimized (7500 steps), allowing full mobility of ligand and side chain atoms but keeping the protein backbone weakly restrained to the template (restraining force constant: 7 kcal mol^{-1} $Å^{-2}$). A dielectric constant of 20 was used to approximately mimic the mixed protein and aqueous environment in the channel region. A relative ranking of the complexes was obtained by subtracting the final complex energies from the energies of the minimized free proteins and ligands.

Results

Inhibition of hEAG1 and hEAG2 Channels by LY97241. hEAG1 channels were shown to be very sensitive to the antiarrhythmic agent clofilium and its sensitivity was similar to that of hERG1 channels (Gessner and Heinemann, 2003). In addition, hEAG1 channels were sensitive to the antiarrhythmic quinidine, whereas hEAG2 channels showed considerably lower sensitivity (Schönherr et al., 2002). Given the potency of clofilium to inhibit hEAG1 channels, we wanted to compare this with hEAG2 to gain a deeper insight into the molecular mechanisms of channel block by antiarrhythmics. Because clofilium is permanently charged and therefore does not readily permeate through the membrane to access the channel pore from the cytoplasmic face, we used its tertiary ammonium analog LY97241, which has been shown to inhibit hEAG1 channels expressed in mammalian cells (Gessner and Heinemann, 2003).

In Fig. 1a, current traces from HEK 293 cells expressing hEAG1 (top) and hEAG2 (bottom) channels are shown for the indicated concentrations of LY97241. hEAG1 channels are already strongly blocked at 10 nM. In contrast, inhibition of hEAG2 channels requires much higher LY97241 concentrations, suggesting a structural difference in the binding sites underlying this difference. The dose-response curves in Fig. 1b yielded apparent IC_{50} values of 10.2 and 1520 nM for hEAG1 and hEAG2, respectively. Thus, under these conditions, hEAG1 channels are inhibited by LY97241 about 150-fold more potently than hEAG2 channels, giving rise to a systematic assessment of the underlying molecular mechanisms.

Chimeras of hEAG1 and hEAG2 Channels. To localize the major molecular determinants for the differences described above, chimeras between hEAG1 and hEAG2 (see *Materials and Methods* and Fig. 2a) were assayed for LY97241 block upon expression in HEK 293 cells. Figure 2b shows dose-response curves for these constructs; the resulting IC_{50} values are presented in Fig. 2c. Introducing the entire core domain of hEAG2 (i.e., all transmembrane segments, including the pore loop) into hEAG1 makes the resulting E1-c2 construct even less sensitive toward LY97241 than hEAG2 (factor 234 with respect to hEAG1). In the reverse case, E2-c1 is not quite as sensitive as hEAG1 (factor 57 with respect to hEAG2). Exchange of the pore regions (E1-p2 and E2-p1) confers the respective properties of the other channel type to a lesser degree (factors 45 and 27, respectively). In contrast, introducing the outer pore region of hEAG2 in hEAG1 (E1-S5p2) had almost no effect (factor 1.6 with respect to hEAG1). For hERG1 it was shown that residues Thr623, Ser624, and particularly Val625, which are conserved in hEAG1 (Thr435, Ser436, and Val437) but differ in part in hEAG2 (Thr431, Thr432, and Ile433) are important for stabilizing the channel blockers MK-499, terfenadine, and cisapride (Mitcheson et al., 2000). Therefore, we also tested the double mutant hEAG1 S436T/V437I (E1-SV/TI) and the

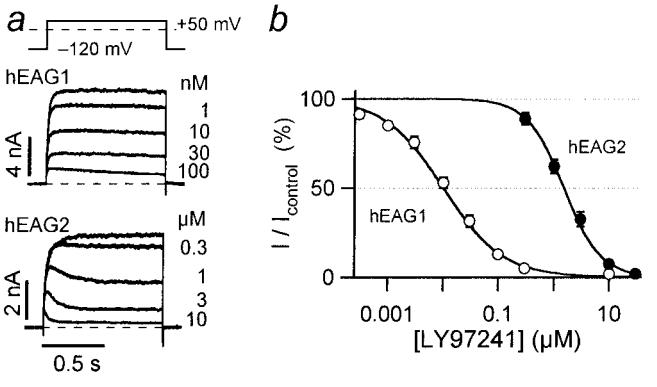

Fig. 1. Inhibition of whole-cell hEAG1 and hEAG2 currents by LY97241. a, superposition of current traces to 50 mV with the indicated concentrations of LY97241. b, dose-response curves of normalized mean data (n = 7–8) with superimposed Hill fits according to the Hill equation under *Materials and Methods*, yielding IC_{50} values of 10.2 ± 0.8 nM and 1.52 ± 0.13 μM for hEAG1 and hEAG2, respectively. The respective Hill coefficients were 0.81 ± 0.03 and 1.30 ± 0.08. Channels were expressed in HEK 293 cells.

reverse mutant hEAG2 T432S/I433V (E2-TI/SV). On a logarithmic scale, both mutants yield roughly intermediate sensitivities between hEAG1 and hEAG2 (factors 33 and 18). Thus, the pore region is the major determinant for LY97241 sensitivity. Residues Ser436 and Val437 in hEAG1 have a strong impact, but they are not the only residues important for stabilization of the ligand. The aromatic residues Tyr464 and Phe468, which were identified to be crucial of MK-499 binding in hERG1 channels (Mitcheson et al., 2000), are conserved among hEAG1, hEAG2, and hERG1 and are thus probably required for drug stabilization but cannot solely account for the high-affinity block of hEAG1 obtained by LY97241.

Voltage Dependence and Activation Kinetics. The block of hEAG1 channels by LY97241 is strongly use- and voltage-dependent (Gessner and Heinemann, 2003). To test whether effects on block efficiency correlate with differences in gating between the EAG variants, we also characterized the voltage dependence and kinetics of activation of all chimeras and mutants. As shown in Fig. 2d, a higher mean open probability is achieved in hEAG1 compared with hEAG2 channels. This could potentially account for the stronger inhibition by the open-channel blocker LY97241. In Fig. 2e, the estimated half-maximal activation voltages (V_n) and the slope factors (k_n) characterizing the voltage dependence of activation are shown for all channel constructs. Chimera E1-c2 has a strongly left-shifted activation ($V_n = -42.7 \pm 2.2$ mV compared with -4.7 ± 2.2 mV for hEAG1). Nevertheless, this left-shift in activation was not accompanied by an increase in block efficiency. In fact, block was even weaker than for hEAG2. The strongest right-shift is observed in chimera E2-p1 ($V_n = 49.6 \pm 1.8$ mV compared with 32.0 ± 3.1 mV for hEAG2). However, block efficiency was intermediate between E2-c1 and E2-TI/SV, both characterized by less depolarized V_n values. Thus, the mutants span a V_n range of about 90 mV, but there is no clear correlation to the block efficiency. A similarly inconsistent picture is obtained for the slope factors, k_n.

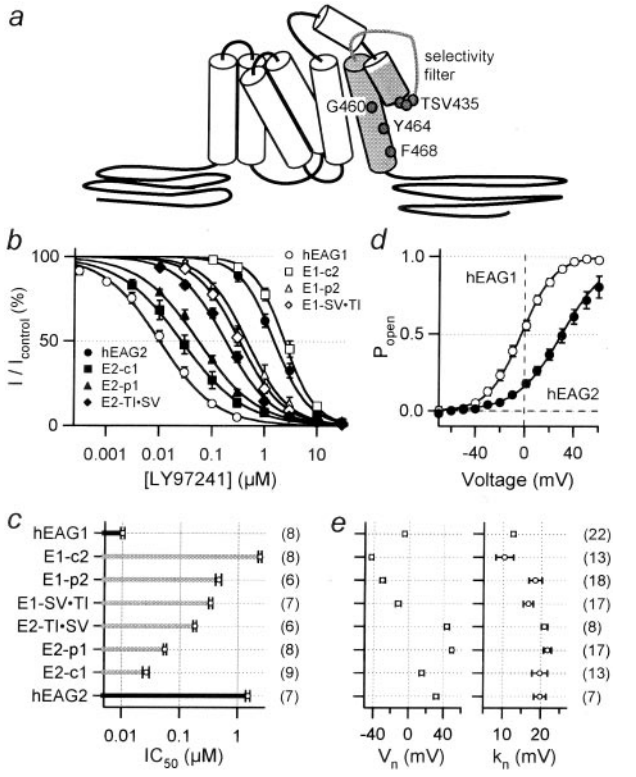

Fig. 2. Chimeric approach to localize clofilium binding. a, cartoon of an hEAG1 subunit indicating the cytoplasmic N- and C-termini (black), the transmembrane core region (all cylinders, S1-S6, residues 183–505 in hEAG1), and the inner pore loop (residues 425–504, gray). Chimeras were constructed between hEAG1 and hEAG2 yielding the channel variants E1-c2, E1-p2, E2-c1, E2-p1. Also indicated are residues TSV435–437, Gly460, Tyr464, and Phe468; the homologous positions in hERG1 channels were shown to be critical determinants for channel block by MK-499 (Mitcheson et al., 2000). b, dose-response relationships of the indicated channel constructs, including the double mutant E1-SV/TI in the background of hEAG1 and the reverse mutant E2-TI/SV in the background of hEAG2, expressed in HEK 293 cells for LY97241. The continuous curves are Hill functions according to the Hill equation under *Materials and Methods*. c, logarithmic presentation of the resulting IC_{50} values for the indicated channel constructs with n in parentheses: hEAG1, 10.2 ± 0.8 nM; E1-c2, 2390 ± 170 nM; E1-p2, 459 ± 51 nM; E1-SV/TI, 334 ± 24 nM; E2-TI/SV, 183 ± 13 nM; E2-p1, 55.3 ± 3.2 nM; E2-c1, 26.6 ± 3.3 nM; hEAG2, 1520 ± 130 nM. d, mean open probability of hEAG1 (○) and hEAG2 (●) obtained from step depolarizations of various voltages and 1 s duration. The continuous curves are fits of Boltzmann functions to the mean normalized data yielding V_n values per channel of -2.6 ± 0.8 mV ($n = 22$) and 30.3 ± 0.5 mV ($n = 7$) for hEAG1 and hEAG2, respectively. The corresponding slope factors k_n were: 13.3 ± 0.5 and 18.2 ± 0.8 mV. e, the mean V_n and k_n values of the wild types and for the remaining channel constructs.

Kinetics of channel activation from hyperpolarized voltages to +50 mV was estimated using a binomial activation model as described previously (Schönherr et al., 1999). This model takes into account the fast and slow gating steps described for the activation of EAG channels. For the time constant of the rapid activation step, hEAG1 (4.15 ± 0.26 ms) and hEAG2 (4.33 ± 0.27 ms) channels did not show significant differences. For the slow activation kinetics, which was about two times faster in hEAG1 (15.1 ± 1.0 ms) than in hEAG2 (27.3 ± 1.7 ms), the core domain was the major determinant (data not shown). The pore domain had an intermediate effect and the double mutation in the pore did not have a big impact. However, these alterations of the gating parameters of the channel constructs did not directly lead to a conclusion regarding residual differences between the block efficiency of hEAG1/E2-c1 and hEAG2/E1-c2, for example.

Thus, differences in susceptibility toward LY97241 between human EAG isoforms cannot be simply explained by their gating characteristics but must result from differences in the binding site within the channel's pore.

Mapping of the Pore by Site-Directed Mutagenesis. Model building of hEAG1 and hEAG2 K^+ channels based on the known structure of the bacterial K^+ channel KcsA indicates that most of the amino acids that differ in both channels do not point toward the interior of the channel (Fig. 3b). Only residues Ser436 (Thr432 in case of hEAG2; see arrow in Fig. 3b) and Val437 (Ile433 for hEAG2) contact the interior of the pore in the models. Replacement of these residues in hEAG1 by the corresponding residues of hEAG2 and vice versa had a strong effect on channel block by LY97241 when expressed in HEK 293 cells.

To gain a better insight into the block mechanism we aimed to measure channel block by direct application of blocker from the cytosolic side. For this purpose, we had to employ *X. laevis* oocytes as an expression system. To avoid any possible ambiguity regarding the binding site, we used clofilium instead of LY97241 for this purpose. The alignment of the pore region of KcsA, hERG1, hEAG1, and hEAG2 (Fig. 3a) shows that only eight residues are different between

hEAG1 and hEAG2 in the inner pore loops. In addition to the double mutant E1-SV/TI we generated all other mutants individually and tested the effect of 10 nM clofilium in inside-out macro-patches. The results are shown in Fig. 3c. Although hEAG2 channels are barely blocked (remaining current, 87.9 ± 2.2%), hEAG1 channel current is reduced to 6.8 ± 0.5% of the control. Most individual mutations, including S491N (data not shown), which in addition to the pore residues differed between hEAG1 and E1-p2, had minor effects when introduced in the background of hEAG1. However, the mutants indicated in red strongly reduced the block by clofilium: S436T (42.9 ± 1.3%), V437I (16.9 ± 1.1%), S436T/V437I (72.2 ± 0.6%), and A453S (41.9 ± 5.6%). Therefore, we can conclude that in addition to the residues Ser436 and Val437 in hEAG1, residue Ala453 contributes to the stabilization of clofilium in the pore.

Comparison of Different Blocking Agents. The impact of Ala453 on channel block by clofilium is not obvious when looking at the structure of the pore model. Previous models in which hERG-blocking substances were docked inside the channel's cavity have considered a contact to sites homologous to Ser436 and Val437 in hEAG1 (Mitcheson et al., 2000). Ala453, however, is not pointing into the pore as reproduced in a molecular modeling approach (see Fig. 3b).

Docking clofilium to the hEAG1 cavity in front of the selectivity filter keeping the protein rigid yielded solutions in which the ligand filled part of the cavity. A typical solution is shown in Fig. 4a (left). The aromatic ring of clofilium is approximately located at the center of the channel contacting the aromatic Phe468 side chains. The corresponding residue (Phe656) has been found previously to be important for high-affinity binding in hERG channels (Mitcheson et al., 2000). However, rigid docking did not produce any placements with close contacts between the ligand and residues that differ between hEAG1 and hEAG2 and that have been found to be important for clofilium binding. In contrast, the semiflexible docking procedure that allowed for conformational relaxation of the protein upon ligand docking (see *Materials and Methods*) resulted in a complex with clofilium in an extended conformation and the alkane tail located in a space between the S6-helix and the selectivity filter. This region is accessible upon small conformational readjustment of the channel structure (Fig. 4a, right). Note that in the crystal structure of an open conformation of the bacterial MthK channel, the space between S6 and the selectivity filter is well accessible (Jiang et al., 2002). In the closed channel form, that is represented by the hEAG1 model, the alkane chain of clofilium is well packed and in van der Waals contact with several hydrophobic groups, among them also Ser436, Val437, and even Ala453 is not very far from the end of the alkane chain (~4 Å). The aromatic part is still in contact with the Phe468 residues located approximately at the center of the channel.

Results from molecular modeling suggest that the alkane tail of clofilium is stabilized in the space between the pore loop and S6, near Ala453. This implies that other blockers without such a tail should not respond strongly to changes at that position. Therefore, we tested the block of hEAG1, hEAG1 S436T, hEAG1 V437I, E1-SV/TI, hEAG1 A453S, and E1-c2 in inside-out patches of *X. laevis* oocytes for block by clofilium, quinidine, and TBA. The chimera E1-c2 was chosen to represent the hEAG2 phenotype, because hEAG2 was expressed only weakly in *X. laevis* oocytes, compromising quantitative measurements in the inside-out mode. The resulting dose-response curves are shown in Fig. 4, a–c (top). The corresponding IC_{50} values are listed in Table 1. In all three cases of blockers, hEAG1 channels are much more strongly inhibited than hEAG2 channels. For clofilium, the difference between hEAG1 and E1-c2 inhibition was smaller by a factor of ~2 than determined in HEK 293 whole-cell measurements, indicating differences in channel gating or block efficiency depending on expression system and recording mode. In addition, in all cases, the double mutant E1-SV/TI strongly reduces the block, almost restoring hEAG2 properties. This is not the case for mutant A453S, however.

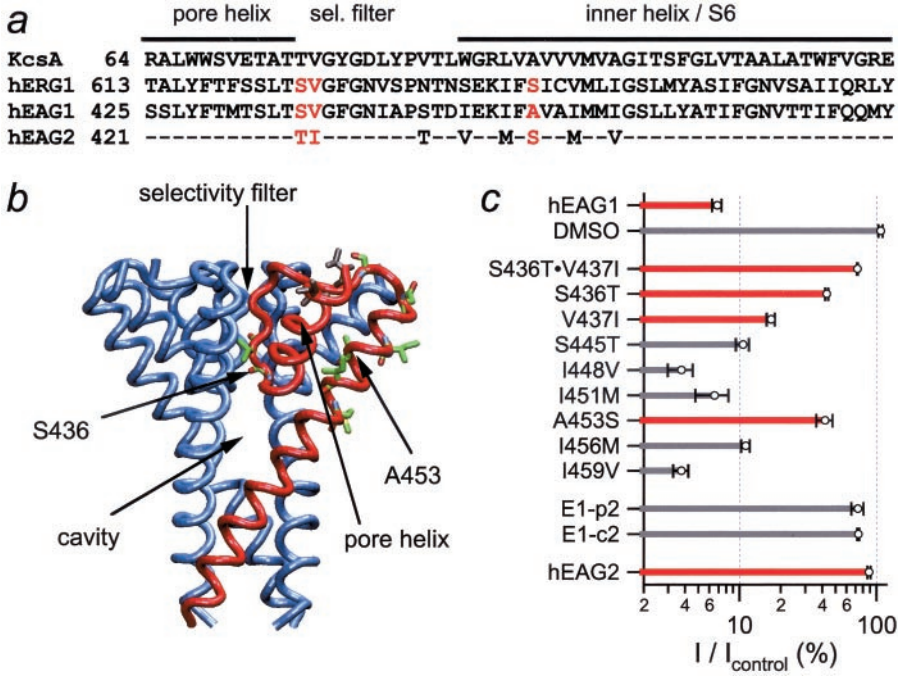

Fig. 3. Molecular differences of hEAG1 and hEAG2 channel pores. a, alignment of the amino acid residues in the pore region of KcsA, hERG1, hEAG1, and hEAG2. Residues identical between hEAG1 and hEAG2 are shown as dashes in the hEAG2 sequence. Within the inner pore loop, there are eight differences between hEAG1 and hEAG2. b, homology model of the tetrameric hEAG1 pore based on a closed structure of KcsA. The backbone of one monomer is shown in red. The side chains of residues that are different in hEAG1 and -2 are shown explicitly (color-coded inside the pore region and gray outside the pore region) for that subunit. c, remaining current at +40 mV (percentage) after application of 10 nM clofilium to inside-out patches from *X. laevis* oocytes expressing the indicated channel constructs. "DMSO" means application of vehicle alone. Red bars highlight the wild types as well as those mutants that reduce clofilium sensitivity most strongly. DMSO, dimethyl sulfoxide.

Although this mutation has a strong impact for clofilium (Fig. 4a), the impact is smaller for quinidine (b) and there is basically no impact at all for TBA (c). With respect to E1-c2, the triple mutant E1-c2-TIS/SVA substantially increases the block efficiency of all substances tested (Table 1).

Subsequently, we attempted to correlate these differences to structural considerations using the docking approach described above. Quinidine can also be docked at a similar position in the cavity, with its aromatic part in contact with the central Phe468 residues. However, it is bulkier than clofilium, and its shorter ethene group cannot penetrate as deeply into the space between the S6-helix and the selectivity filter as clofilium (see Fig. 4b). The interaction between the channel blockers clofilium and quinidine with the hEAG1 variants was calculated after conformational relaxation of the mutated model complexes (Table 1). Mainly because of an increased sterical strain caused by the larger side chains Thr432 and Ile433 (hEAG2 numbering) in two of the variants, a reduced ranking compared with wild-type hEAG1 was found in qualitative agreement with the experimental observation. In the reverse case the double mutation in the background of hEAG2 (E2-TI/SV) enhanced clofilium binding by about the same energy difference (−9.2 kcal/mol) than obtained for E1-SV/TI (+10.8 kcal/mol; see Table 1). The distance (>10 Å) between the ligand and amino acids 445, 448, 451, 456, and 459 excluded any sterical influence on clofilium binding in these calculations. No effect or only a very small calculated effect was found for the A453S mutant, indicating

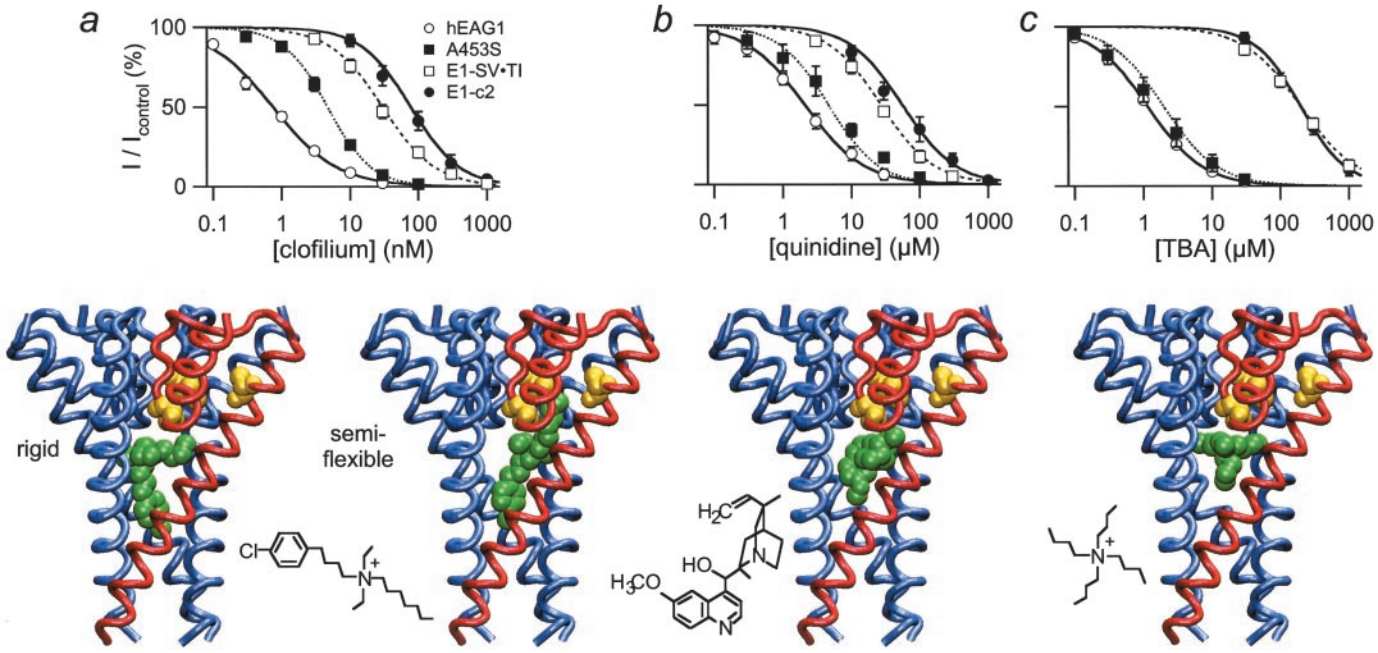

Fig. 4. Dose-dependent block of hEAG1 and mutants by clofilium, quinidine, and TBA. Top, dose-response data for the indicated blockers were compiled in inside-out patches from *X. laevis* oocytes, with 1-s pulses to +50 mV. Each plot contains data for hEAG1 wild-type (○), mutants A453S (■), and S436T/V437I (□) and chimera E1-c2 (●). Continuous curves are results of fits to the Hill equation under *Materials and Methods*; the results are listed in Table 1. Bottom, putative ligand binding geometries at the central channel cavity obtained after docking of clofilium (a), to a rigid (left) and to a semiflexible (right) hEAG1 model structure. b, a placement for quinidine after docking to a semiflexible channel model. c, the binding placement obtained for TBA is based on the X-ray structure of TBA in complex with the KcsA (see *Materials and Methods*). Only the backbones of the channel models (blue and one subunit in red) are shown. The ligands (green) and residues Ala453, Ser436, and Val437 (yellow) are indicated as van der Waals spheres. In addition, the chemical structures of the ligands are shown.

TABLE 1

Comparison of channel block and calculated ligand binding energies

For each blocking agent the first column shows for the indicated mutants IC_{50} values obtained at +50 mV in inside-out patches of *X. laevis* oocytes. The Hill coefficients of the corresponding dose-response curves were all in the range of 0.8 to 1.2 and are not shown here. The next column shows estimates for the changes in energy when mutants were introduced with a docked blocker molecule in place.

	Clofilium			Quinidine		TBA
Mutant	IC_{50}	ΔE_{bind} fl.	ΔE_{bind} ri.	IC_{50}	ΔE_{bind} fl.	IC_{50}
	nM (n)	*kcal/mol*	*kcal/mol*	*μM (n)*	*kcal/mol*	*μM (n)*
hEAG1	0.79 ± 0.09 (5)	0.0	0.0	2.08 ± 0.36 (5)	0.0	1.15 ± 0.07 (4)
S436T	7.87 ± 0.76 (6)	9.5	−0.5	3.90 ± 0.80 (4)	5.1	68.4 ± 4.6 (5)
V437I	3.04 ± 0.41 (4)	1.5	0.6	5.77 ± 0.39 (6)	4.5	5.96 ± 0.25 (5)
S436T/V437I	30.0 ± 4.4 (6)	10.8	−0.7	27.2 ± 4.7 (6)	4.1	198 ± 23 (6)
A453S	4.67 ± 0.50 (5)	0.6	0.2	4.60 ± 1.27 (7)	0.1	1.97 ± 0.68 (5)
E1-c2	77.3 ± 19.2 (5)			55.6 ± 13.7 (7)		198 ± 33 (5)
E1-c2 TIS/SVA	7.90 ± 0.95 (6)			7.27 ± 0.41 (5)		12.5 ± 1.3 (5)
S433A	1.48 ± 0.20 (6)			0.31 ± 0.06 (5)		0.089 ± 0.011 (5)
S433C	0.60 ± 0.08 (5)			0.39 ± 0.01 (4)		0.29 ± 0.09 (5)

ΔE_{bind} fl., energy for clofilium and quinidine at a position obtained from semiflexible docking shown in Fig. 4, a, right, and b; ΔE_{bind} ri., energy for clofilium located at a position obtained after rigid docking (Fig. 4a, left).

that there may not be sterical reasons for the observed reduction in binding of this variant. Ligand docking studies, including explicit water molecules, are computationally too demanding to allow for a systematic search for putative ligand binding positions at the channel pore region. Therefore, polar and electrostatic contributions to the calculated ranking of docking solutions have been included approximately by applying an implicit electrostatic screening model with an effective dielectric constant $\epsilon = 20$ (representing the mixed protein and aqueous environment in the pore). The nonpolar alkane chain of clofilium forms a well packed complex with the "anchor" region in the docked complexes such that the relative ranking is mainly determined by the sterical fitness between channel mutants and ligand.

However, it might be possible that the A453S mutation stabilizes or traps water molecules (not present in the calculations) in the space between the S6-helix and the selectivity filter that must be expelled by hydrophobic groups of the ligands. Such effects are not included in the calculated ranking of ligand binding. The calculated ranking in case of a docking position obtained after rigid docking (with no close contacts between Ser436 or Val437 and clofilium) (Fig. 4a) showed a much smaller effect of the mutations on binding with no correlation to the experimental results (Table 1).

Based on the X-ray structure of the KcsA channel in complex with TBA, a model for the hEAG1-TBA complex was generated (see *Materials and Methods*). In this model, the quaternary ammonium group of TBA is located at the entrance of the selectivity filter and the butyl groups partly filling the cavity but without close contacts to Ser436, Val437, or Ala453 (Fig. 4c). For this binding geometry, no significant sterical influence was found on mutation of the above residues on binding (data not shown). However, more accurate electrostatic energy calculations using the finite-difference Poisson-Boltzmann method (Madura et al., 1995) indicate a higher electrostatic penalty for introducing TBA into an S436T cavity compared with wild-type hEAG1. In the finite-difference Poisson-Boltzmann method, a dielectric boundary between molecule and surrounding aqueous solvent is introduced, allowing estimation of the change in electrostatic solvation upon complex formation. In case of TBA binding to the smaller S436T cavity, the calculated change in electrostatic solvation was 2.1 kcal/mol less favorable than binding to the wild-type hEAG1 cavity assuming an internal dielectric constant $\epsilon_{in} = 4$. This difference increased to 4.9 kcal/mol in case of using $\epsilon_{in} = 2$ for the protein ($\epsilon_w = 78$ for water). Such energy changes correspond to changes of the binding constant of between 30 ($\epsilon_{in} = 4$) and 3500 ($\epsilon_{in} = 2$) in qualitative agreement with the experimental observation of strongly reduced TBA binding to hEAG2 or hEAG1 variants that contain an S436T mutation.

Thus, with the semiflexible docking approach, we were able to qualitatively explain the molecular mechanisms underlying the differences in efficiency of block by clofilium, quinidine, and TBA. The data suggest that a possible anchoring of hydrophobic chains of blocking molecules in the cavities between the pore helix and S6 can result in additional stabilization yielding high-affinity block.

Because the impact of mutation A453S on the effect of clofilium could be circumstantial, we tested as additional hERG1 channel blockers MK-499 and terfenadine for their efficiency to inhibit currents mediated by hEAG1, hEAG1 A453S, and E1-c2. In inside-out patches, the following IC_{50} values were determined: MK-499, 102 ± 14 nM ($n = 4$, hEAG1), 358 ± 30 nM ($n = 5$, A453S), 22.7 ± 1.5 μM ($n = 5$, E1-c2); terfenadine, 15.8 ± 2.6 nM ($n = 6$, hEAG1), 177 ± 14 nM ($n = 3$, A453S), 1.03 ± 0.24 μM ($n = 3$, E1-c2). Thus, both substances distinguish well between hEAG1 and hEAG2 pores (factor of 222 and 65, respectively) and in both cases, mutation A453S has a significant effect on channel block (factor of 3.5 and 11.2, respectively).

The obvious effect of mutation A453S on the channel block by clofilium, quinidine, MK-499, and terfenadine suggests that neighboring residues may also affect drug stability in the pore. Therefore, we attempted to assay mutation M457A, a structural neighbor of Ala453 located closer to the pore cavity. This mutant resulted only in very small currents in *X. laevis* oocytes that could not be assayed with patch-clamp methods. In addition, the small currents measured in whole oocytes displayed inactivation such that a faithful interpretation of block studies would be compromised. Residue Ser433 is located on the pore helix in relation to the center between Ala453 and M457. When mutated to either alanine or cysteine, channels with largely normal kinetics were obtained. The block by clofilium in the inside-out configuration was affected only marginally (less than 2-fold; see Table 1). This result is compatible with model considerations because neither S433A nor S433C has a strong sterical impact on the alkane chain of clofilium when located in the pore pocket. Channel block by quinidine and terfenadine was strongly increased (4- to 13-fold reduced IC_{50} values; see Table 1), supporting the importance of the pore pocket region in stabilizing drugs inside the hEAG pore. However, with the modeling approach applied here, the increased binding of TBA and quinidine is not readily explained.

Discussion

The acquired form of the long-QT syndrome is a relatively common side effect of therapeutically different drugs (Keating and Sanguinetti, 2001). The hERG1 potassium channels, which give rise to the repolarizing I_{Kr} currents in cardiac myocytes, are the primary molecular targets. Several studies have shown that, compared with Kv channels, the outstanding pharmacological sensitivity of the hERG1 channels is mainly based on a larger volume of the inner cavity forming the binding site (del Camino et al., 2000; Mitcheson et al., 2003), and the lining of this binding site in particular by two aromatic residues (Tyr652 and Phe656) within S6 (Mitcheson et al., 2000). Moreover, inactivation of hERG1 channels strongly enhances the block efficiency of several drugs (e.g., Suessbrich et al., 1997; Ficker et al., 1998, 2001), although the underlying mechanism is not fully understood (Chen et al., 2002). In this work, we studied the inhibition of a pair of channels, hEAG1 and hEAG2, that, in contrast to hERG1 channels, do not inactivate but share the important aromates and the large size of the inner cavity with hERG1 channels. Although several drugs block hEAG1 and hERG1 channels in a similar fashion, hEAG2 channels are often much less sensitive. Therefore, the couple hEAG1/hEAG2 constitutes an ideal pair of ion channels suited to study the molecular details involved in high-affinity block of EAG channels in general but in the absence of inactivation.

Channel Inhibition by LY97241. hEAG1 channels expressed in HEK 293 cells are effectively blocked by LY97241, a tertiary analog of the antiarrhythmic agent clofilium (Steinberg and Molloy, 1979). The IC_{50} value of 10.2 nM obtained in this study agrees well with previous studies on hEAG1 channels expressed in Chinese hamster ovary cells (4.9 nM) and HEK 293 cells (8.3 nM), measured with a similar pulse protocol, but in the presence of physiological Mg^{2+} concentrations (Gessner and Heinemann, 2003). hEAG2 channels, which like hEAG1 channels do not inactivate, are much less effectively blocked by LY97241. The slightly weaker inhibition of hEAG1 compared with hERG1 channels (2.2 nM) might reflect the lack of inactivation, which was shown to affect hERG inhibition by LY97241 (Suessbrich et al., 1997) and other blockers like dofetilide (Ficker et al., 1998, 2001). The difference in LY97241 sensitivity between hEAG1 and hEAG2 (150-fold), which clearly is not attributable to differences in channel gating, is slightly larger than for quinidine [100-fold (Schönherr et al., 2002)]. In both cases, the IC_{50} values for the inhibition of hEAG1 channels are less than 5-fold higher than for hERG1 channels (Paul et al., 2002; Gessner and Heinemann, 2003). Thus, the pharmacological differences between the two noninactivating channels hEAG1 and hEAG2 are much more pronounced than between hEAG1 and the inactivating channel hERG1. The same holds true for the two hERG blockers terfenadine and MK-499, which block hEAG1 with a potency intermediate to those of clofilium and quinidine. Introduction of the hEAG2 core into the hEAG1 channel reduced the effects of all substances tested by at least 50-fold.

The potency of LY97241 to inhibit either channel is about 100-fold higher than for quinidine. Previous work on EAG channels has been hampered by the lack of potent and selective blocking agents. Therefore, the finding that LY97241, clofilium, and terfenadine are high-affinity blockers for hEAG1 is of high practical relevance. Because EAG1 channels have been implied to increase the oncogenic potential of tumor cells (Pardo et al., 1999), pharmacological tools are urgently needed to test this hypothesis and to examine the usefulness of these channels as pharmacological targets in cancer treatment. In addition, these blockers may be useful tools to distinguish EAG1 and EAG2 channels in the central nervous system to elucidate their physiological role in neuronal signaling.

Molecular Mechanism of Clofilium Block. Building on the similarities between LY97241 and clofilium in structure and their binding to hEAG1 channels (Gessner and Heinemann, 2003), we tested the effect of single-site mutations in hEAG1 on clofilium block. To gain direct access of the blocker to the intracellular side, channels were expressed in *X. laevis* oocytes, and clofilium was applied in the inside-out configuration. Note that the stronger effect of clofilium in these experiments, compared with the channel inhibition by LY97241 in HEK 293 cells, can be explained by the different recording modes (whole-cell versus inside-out) and a slightly higher potency of clofilium compared with LY97241 (Gessner and Heinemann, 2003).

We found that three residues in hEAG1 (Ser436, Val437, and Ala453), when mutated to the corresponding residues in hEAG2, attenuated clofilium block. The other residues have only marginal impact because they are apparently not pointing toward the pore pocket (e.g., I456M and I459V). Two of the important residues (Ser436 and Val437) located at the apex of the pore helix and, hence, lining the inner cavity are conserved in hERG1 channels and also affected hERG1 channel inhibition by MK-499 when mutated to alanine (Mitcheson et al., 2000). In agreement with our results for LY97241 block, a double mutation of both residues does not fully confer clofilium sensitivity between hEAG1 and hEAG2 channels. The third residue, Ala453, remote from the inner cavity, also attenuates clofilium block, intermediate to the single-site mutations at positions 436 and 437. Residue Ala453 also strongly affects binding of MK-499 and terfenadine although channel block by TBA is not altered.

To interpret the experimental findings on a molecular and structural level we employed docking studies of clofilium to homology models of hEAG1 and hEAG2 channels, based on the crystal structure of the bacterial KcsA channel. The modeling attempt is based on the assumption that the channel structure of KcsA is generally similar to that of the hEAG1 and hEAG2 structures. Although the resulting structural models showed good stereochemical quality, such homology models may contain structural inaccuracies (e.g., small misplacements of main chain and side chain elements), possibly limiting its usefulness for docking studies. In fact, using the rigid model structures during docking forced clofilium to adopt a kinked conformation (a typical solution is shown in Fig. 4a) to fit into the space in front of the selectivity filter, and the resulting model was unable to explain the experimental findings. To cope with the possible inaccuracies of the homology models and the possibility of protein conformational changes during ligand binding, we employed a semiflexible docking procedure. This procedure allowed for full relaxation of protein side chains and at least partial adjustment of main chain and whole secondary structural elements during docking. The semiflexible docking procedure resulted in a clofilium-channel complex with intimate contacts between clofilium and residues 436 and 437, and the alkane tail of clofilium located in a space between S6 and pore helix, a working model referred to as anchored cavity block. In addition to the larger number of contacts with the protein, the clofilium ligand adopts an energetically more favorable straight conformation with most dihedral torsion angles of the alkane chain in the trans configuration compared with the conformations observed in case of rigid docking. The ligand placement found assuming a semiflexible protein during docking is further supported by the qualitative agreement of calculated ranking versus experimental data for amino acid substitutions at residues 436 and 437 (see below). Moreover, the aromate ring of clofilium is in close contact to the aromatic Phe468 side chain, presumably determining the enhanced block efficiency compared with Kv channels (Malayev et al., 1995). The corresponding residue (Phe656) has been shown previously to be important for high-affinity binding in hERG channels (Mitcheson et al., 2000). Phe468, however, cannot account for the difference in clofilium block between hEAG1 and hEAG2 channels because it is conserved between both channel isoforms.

The ligand docking performed in this study assumed an ideal fit of the ligand in the closed channel conformation, because there is ample of evidence that high-affinity blockers, particularly clofilium (Gessner and Heinemann, 2003), are trapped in the closed channel. However, it should be noted that the open-channel conformation provides a much

greater room for potential blocking molecules such that the initial association to the docking site can be much facilitated.

Anchored Cavity Block. The strong effect of the A453S mutation on clofilium block of hEAG1 channels may be explained either as a direct effect on the proposed alkane tail binding site or an indirect gating effect, caused by an altered flexibility of the S6 helices. To discriminate between these possibilities, we compared the effect of mutations at positions 436, 437, and 453 on EAG inhibition by clofilium, quinidine, and TBA. In addition, we tested the effect of A453S on MK-499 and terfenadine block. Although anchored binding was expected to be weaker for quinidine, because of a bulkier and shorter alkane side chain, no anchored binding should be observable for TBA. Moreover, docking simulations supported the experimentally testable hypothesis that the strength of attenuation of block by mutations at positions 436 and 437 should be in the order 436 $>$ 437 for clofilium, 436$\approx$437 for quinidine, and 436 $\gg$ 437 for TBA, although in the latter case attributable more to electrostatic than sterical reasons. The experimental results were in good agreement with these presumptions. In addition, MK-499 and terfenadine might be able to protrude into the pore pocket. However, as modeled for MK-499 to a closed channel structure (data not shown), more space is required between S6 and the pore helix to accommodate the bulkier tails. It is readily conceivable, however, that this space is provided in a fully flexible channel given the large conformational changes expected during channel opening (Jiang et al., 2002).

Hence, in addition to the aromatic residues Tyr464 and Phe468, which were postulated to stabilize antiarrhythmic agents in the pore of hERG1 channels by a π-stacking mechanism, more requirements are necessary for high-affinity block of K^+ channels of the EAG family. Our data suggest that a possible anchoring of hydrophobic chains of blocking molecules in the cavities between the pore helix and S6 can result in additional stabilization yielding high-affinity block. Such additional interactions between alkyl tails and parts of the pore wall have been postulated also for block of Kv channels by alkyl-triethylammonium derivatives (Choi et al., 1993), depending on the length of the alkyl chains. Future studies, using trifunctional, clofilium-based substances with different lengths and flexibilities of the alkyl-tail and the alkyl-linker to the aromate head, have to address the exact positioning of clofilium within the EAG channel cavity. This is important because 1) aromatic groups, as in dofetilide, may permit such an anchoring (Ficker et al., 2001) and 2) the homologous position of the S6 aromates between human ERG1 and *Drosophila melanogaster* EAG1 has been questioned and repositioning during activation/inactivation gating may occur (Chen et al., 2002).

Our proposed model of anchored cavity block for substances like clofilium explains the pharmacological differences between hEAG1 and hEAG2 channels. However, it cannot be excluded that allosteric effects induced by changes at position Ala453 contribute to the observed phenotypes. Nevertheless, regardless of the exact molecular binding mode, the results provided here highlight for the first time the importance of residues in the space between S6 and the pore helix for the stabilization of various drugs in the pore of EAG channels.

Given the clinical relevance, a natural question is whether or not the equivalent sites would also affect pore block of hERG1 channels. hERG1 channels harbor a serine at that position (Ser641). We generated mutation hERG1 S641A and assayed it for block by LY97241, quinidine, and MK-499 in HEK 293 cells. The block by LY97241 was increased by a factor of 2 (wt, 2.17 $\pm$ 0.44 nM, n = 5; mutant, 1.03 $\pm$ 0.04 nM, n = 6). The block of quinidine (1.27 $\pm$ 0.46 μM, n = 5 versus 1.38 $\pm$ 0.15 μM, n = 5) and MK-499 (7.78 $\pm$ 1.29 nM, n = 5 versus 11.6 $\pm$ 1.7 nM, n = 6) was not affected. This result qualitatively supports the impact of residue S641 for the stabilization of LY97241 in hERG1 channels. However, mutation S641A accelerates inactivation by about 4 to 5-fold and shifts the midpoint of voltage-dependence of recovery from inactivation by about $-$40 mV. Therefore, a faithful quantitative assessment of state-independent binding properties of the blockers cannot be achieved. In fact, this is one of the major advantages of using the hEAG1 channel as a model system for such studies, because its pore is highly homologous to that of hERG1 channels but does not undergo inactivation.

Because block of hERG1 channels is often the cause of undesired cardiac drug side-effects, pharmacophore models would be valuable for the estimation of hERG1 inhibition by compounds before expensive preclinical and clinical studies. However, recent attempts to create such models were based on the assumption that compounds in the pore cavity are bound by a common mechanism (Ekins et al., 2002). Our structural consideration for hEAG channels now imply that small compounds such as TBA are bound by the cavity, whereas affinity to alkyl-tailed compounds, such as clofilium, or substances with bulkier tails, such as MK-499 and terfenadine, can be increased by neighboring pore compartments. Regardless of whether this relies on direct anchoring of the drugs in the pore pocket, one can distinguish between (at least) two groups of blockers with different binding modes, being affected by either mutation A453S or S433A in hEAG1. Because different binding modes imply different drug–channel interactions, it seems likely that one cannot straightforwardly propose a universal pharmacophore model for hERG (or hEAG) channels. Predictive pharmacophore models for the EAG channel family need to account for different binding modes of complex blocker structures.

Acknowledgments

We are grateful for technical assistance by S. Arend and A. Rossner.

References

Bauer CK and Schwarz JR (2001) Physiology of EAG K^+ channels. *J Membr Biol* **182:**1–15.

Case DA, Pearlman DA, Caldwell JW, Cheatham TE, Ross WS, Simmerling CL, Darden TA, Merz KM, Stanton RV, Cheng AL, et al. (1999) AMBER 6. University of California, San Francisco.

Chen J, Seebohm G, and Sanguinetti MC (2002) Position of aromatic residues in the S6 domain, not inactivation, dictates cisapride sensitivity of HERG and eag potassium channels. *Proc Natl Acad Sci USA* **99:**12461–12466.

Choi KL, Mossman C, Aubé J, and Yellen G (1993) The internal quaternary ammonium receptor site of Shaker potassium channels. *Neuron* **10:**533–541.

Doyle DA, Morais Cabral J, Pfuetzner RA, Kuo A, Gulbis JM, Cohen SL, Chait BT, and MacKinnon R (1998) The structure of the potassium channel: molecular basis of K^+ conduction and selectivity. *Science (Wash DC)* **280:**69–77.

del Camino D, Holmgren M, Liu Y, and Yellen G (2000) Blocker protection in the pore of a voltage-gated K^+ channel and its structural implications. *Nature (Lond)* **403:**321–325.

Ekins S, Crumb WJ, Sarazan D, Wikel JH, and Wrighton SA (2002) Three-dimensional quantitative structure-activity relationship for inhibition of human ether-a-go-go-related gene potassium channel. *J Pharmacol Exp Ther* **301:**427–434.

Ficker E, Jarolimek W, Kiehn J, Baumann A, and Brown AM (1998) Molecular determinants of dofetilide block of HERG K^+ channels. *Circ Res* **82:**386–395.

Ficker E, Jarolimek W, and Brown AM (2001) Molecular determinants of inactivation and dofetilide block in ether a-go-go (EAG) channels and EAG-related K^+ channels. Mol Pharmacol **60:**1343–1348.
Gessner G and Heinemann SH (2003) Inhibition of hEAG1 and hERG1 potassium channels by clofilium and its tertiary analogue LY97241. *Br J Pharmacol* **138:** 161–171.
Ho SN, Hunt HD, Horton RM, Pullen JK, and Paese LR (1989) Site-directed mutagenesis by overlap extension polymerase chain reaction. *Gene* **77:**51–59.
Jiang Y, Lee A, Chen J, Cadene M, Chait BT, and MacKinnon R (2002) The open pore conformation of potassium channels. *Nature (Lond)* **417:**523–526.
Ju M and Wray D (2002) Molecular identification and characterisation of the human eag2 potassium channel. *FEBS Lett* **524:**204–210.
Kamiya K, Mitcheson JS, Yasui K, Kodama I, and Sanguinetti MC (2001) Open channel block of HERG K^+ channels by vesnarinone. *Mol Pharmacol* **60:**244–253.
Keating MT and Sanguinetti MC (2001) Molecular and cellular mechanisms of cardiac arrhythmia. *Cell* **104:**569–580.
Lees-Miller JP, Duan Y, Teng GQ, and Duff HJ (2000) Molecular determinant of high-affinity dofetilide binding to HERG1 expressed in Xenopus oocytes: Involvement of S6 sites. *Mol Pharmacol* **57:**367–374.
Madura JD, Briggs JM, Wade RC, Davis ME, Luty BA, Ilin A, Antosiewicz J, Gilson MK, Bagheri B, Scott LR, and McCammon JA (1995) Electrostatics and diffusion in solution: simulations with the University of Houston Brownian Dynamics program. *Comput Phys Commun* **91:**57–95.
Malayev AA, Nelson DJ, and Philipson LH (1995) Mechanism of clofilium block of the human Kv1.5 delayed rectifier potassium channel. *Mol Pharmacol* **47:**198–205.
Milnes JT, Crociani O, Arcangeli A, Hancox JC, and Witchel HJ (2003) Blockade of HERG potassium currents by fluvoxamine: incomplete attenuation by S6 mutations at F656 or Y652. *Br J Pharmacol* **139:**887–898.
Mitcheson JS, Chen J, Lin M, Culberson C, and Sanguinetti MC (2000) A structural basis for drug-induced long QT syndrome. *Proc Natl Acad Sci USA* **97:**12329–12333.
Mitcheson JS (2003) Drug binding to HERG channels: evidence for a 'non-aromatic' binding site by fluvoxamine. *Br J Pharmacol* **139:**883–884.
Pardo LA, del Camino D, Sanchez A, Alves F, Brüggemann A, Beckh S, and Stühmer W (1999) Oncogenic potential of EAG K^+ channels. *EMBO (Eur Mol Biol Organ J) J* **18:**5540–5547.
Paul AA, Witchel HJ, and Hancox JC (2002) Inhibition of the current of heterologously expressed HERG potassium channels by flecainide and comparison with quinidine, propafenone and lignocaine. *Br J Pharmacol* **136:**717–729.
Sánchez-Chapula JA, Navarro-Polanco RA, Culberson C, Chen J, and Sanguinetti MC (2002) Molecular determinants of voltage-dependent human ether-a-go-go related gene (HERG) K^+ channel block. *J Biol Chem* **277:**23587–23595.
Sanguinetti MC, Jiang C, Curran ME, and Keating MT (1995) A mechanistic link between an inherited and an acquired cardiac arrhythmia: HERG encodes the I_{Kr} potassium channel. *Cell* **81:**299–307.
Schönherr R, Gessner G, Löber K, and Heinemann SH (2002) Functional distinction of human EAG1 and EAG2 potassium channels. *FEBS Lett* **514:**204–208.
Schönherr R, Hehl S, Terlau H, Baumann A, and Heinemann SH (1999) Individual subunits contribute independently to slow gating of bovine EAG potassium channels. *J Biol Chem* **274:**5362–5369.
Schönherr R and Heinemann SH (1996) Molecular determinants for activation and inactivation of HERG, a human inward rectifier potassium channel. *J Physiol* **493:**635–642.
Steinberg MI and Molloy BB (1979) Clofilium—a new antifibrillatory agent that selectively increases cellular refractoriness. *Life Sci* **25:**1397–1406.
Suessbrich H, Schönherr R, Heinemann SH, Lang F, and Busch AE (1997) Specific block of cloned Herg channels by clofilium and its tertiary analog LY97241. *FEBS Lett* **414:**435–438.
Zhou M, Morais-Cabral JH, Mann S, and MacKinnon R (2001) Potassium channel receptor site for the inactivation gate and quaternary amine inhibitors. *Nature (Lond)* **411:**657–661.

Address correspondence to: Prof. Dr. Stefan H. Heinemann, Molecular and Cellular Biophysics, Friedrich Schiller University Jena, Drackendorfer Str. 1, D-07747 Jena, Germany. E-mail: stefan.h.heinemann@uni-jena.de